Dual-Domain Regulation of Dissolved Organic Matter Release in Soil: The Role of pH and Calcium

Hui Gao, Liping Weng,* Rob N. J. Comans, and Gerwin F. Koopmans



Downloaded via WAGENINGEN UNIV & RESEARCH on July 2, 2025 at 12:18:54 (UTC). See https://pubs.acs.org/sharingguidelines for options on how to legitimately share published articles.

Cite This: ACS Earth Space Chem. 2025, 9, 1377-1391



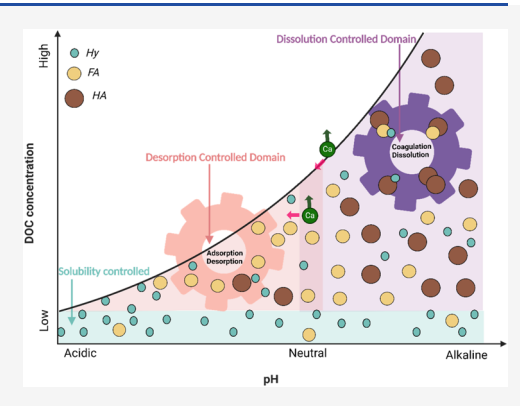
ACCESS I

III Metrics & More

Article Recommendations

s Supporting Information

ABSTRACT: Dissolved organic matter (DOM), being the most reactive soil organic matter (SOM) fraction, affects key biogeochemical processes in soil like nutrient cycling, pollutant transport, and organic carbon sequestration. Quantitative understanding of physical-chemical processes regulating the release of DOM in response to variation in factors such as pH and Ca concentration is still lacking. Here, we conducted batch experiments and employed the Natural Organic Matter-Charge Distribution (NOM-CD) model and the Non-Ideal Consistent Competitive Adsorption-Donnan (NICA-Donnan) model to investigate the physical-chemical processes controlling DOM release in seven agricultural topsoils under varying pH (3-9) and Ca concentration (0-10 mM). The DOM fractionation results showed that while hydrophilic acid (Hy), fulvic acid (FA), and humic acid (HA) concentrations increased with pH, their contribution to total DOM differed: Hy and HA dominated at respectively low pH



 $(\sim 4-6)$ and high pH $(\sim 8-9)$, whereas FA peaked at near-neutral pH $(\sim 6.5-7)$. Our NOM-CD model calculations revealed that changes in the DOM concentration at low pH (pH < \sim 5-6.5) were mainly due to OM desorption from soil minerals. Changes in the DOM concentration at high pH (pH > \sim 5-6.5) were predominantly controlled by OM dissolution, as demonstrated by the relation between the DOM concentration and Donnan potential (φ_D) of DOM calculated with the NICA-Donnan model. Based on these findings, we propose a conceptual Dual-Domain Desorption Dissolution model in which the relative importance of these two controlling mechanisms is quantitatively assessed for the first time. These insights will be helpful to better quantify soil management effects on the stability and functioning of SOM.

KEYWORDS: soil organic matter, dissolved organic carbon, chemical fractionation, supramolecule, carbon sequestration, surface complexation modeling

1. INTRODUCTION

Dissolved organic matter (DOM), being the most mobile and active fraction of soil organic matter (SOM), consists of various compounds derived from plant litter, root exudates, and microbial biomass, varying in different stages of degradation. 1-3 The release of DOM from soil to solution exerts a substantial influence on a diverse array of biogeochemical processes in soil such as cycling of carbon, nitrogen, and phosphorus as well as the transport of these nutrients to aquatic ecosystems where they can contribute to eutrophication.⁴⁻⁷ Furthermore, DOM facilitates the transport of pollutants such as heavy metals, pesticides, microplastics, and polyfluoroalkyl substances (PFAS). For instance, adsorption of DOM onto microplastic surfaces can potentially increase their hydrophilicity and enhance their mobility.8 Likewise, the interaction between DOM and PFAS, either via a competition effect for binding to reactive surfaces of soil metal-(hydr)oxides or via the formation of soluble DOM-PFAS complexes, can enhance the mobility of these pollutants.^{9,10} Soil is the largest terrestrial carbon pool and plays a key role in the global carbon cycle. 11,12 However, over the past decades, a

decrease in SOM and a concomitant increase in the concentration of DOM in surface waters have been observed in Europe and North America. 13-15 These observations have been linked to a reduction in atmospheric acid deposition and soil-calcium (Ca) depletion as a key factor in decreasing the ionic strength of soil solution. 14,16 Hence, a thorough understanding of the processes governing the release of DOM from soil is crucial to support the development of measures to mitigate losses of DOM and associated pollutants from soil to aquatic ecosystems and to enhance soil organic carbon sequestration.

Dissolved organic matter comprises complex and heterogeneous compounds with a range in molecular weight and other properties such as charge, aromaticity, and hydrophobicity. 17,18

Received: December 6, 2024 Revised: May 9, 2025 Accepted: May 9, 2025 Published: May 21, 2025





Dissolved organic matter has been operationally fractionated into humic acids (HA), fulvic acids (FA), hydrophobic neutrals (HON), and hydrophilic compounds (Hy), based on their pHdependent hydrophilic and hydrophobic properties. 19 Despite the debate regarding the existence of these fractions in soils, their properties do well reflect the heterogeneity of SOM.^{20,2} The generally observed variation in the relative contribution of these fractions to total DOM for soils with different properties^{22,23} may reflect different mechanisms dominating their release to solution. Within these fractions, FA and HA can interact strongly with soil metal-(hydr)oxides due to their high density of carboxylic- and phenolic-type functional groups, which strongly influences adsorption of oxyanions (e.g., phosphate) to these reactive surfaces as a result of competition. The HON fraction is more hydrophobic than FA and is often quantified together with FA in fractionation procedures. ^{22,28} Among all DOM fractions, Hy is the most soluble fraction due to its low molecular weight, and is more mobile in leaching processes. The Hy fraction consists of various types of easily soluble organic compounds, such as low molecular weight organic acids, amino acids, sugar, and proteins.²⁹ Specific hydrophilic acids like citric acid have been observed to adsorb onto soil oxides, 30 similar to FA and HA. At low pH or in the presence of multivalent cations, HA can coagulate and precipitate.³¹ The formation of supramolecular arrangements has recently been proposed to play an important role in determining the structure and properties of humic SOM fractions in which different components of relatively low molecular mass form larger organic matter (OM) associations through hydrophobic interactions, cation bridges, and H-bonds. 32,33 The formation of these supramolecular associations, influenced by soil properties like pH and the presence of multivalent cations, ^{34,35} likely contributes to the adsorption and coagulation processes of OM, which, in turn, control DOM formation and release.

Surface complexation modeling (SCM) is a sophisticated approach to simulate the physical-chemical processes describing the binding of ions at the surface of mineral and organic adsorbents. For instance, the Natural Organic Matter-Charge Distribution (NOM-CD) model²⁵ has been developed to incorporate the effects of natural organic matter (NOM) on ion adsorption to minerals. By simulating solid-solution distribution of phosphate, the amount of NOM adsorbed in the compact part of electric double layer (EDL) can be calculated. ^{25,39} On the other hand, the Non-Ideal Consistent Competitive Adsorption-Donnan (NICA-Donnan) model³ can be applied to describe the properties of humic substances in relation to variation in pH, solution composition, and specifically and nonspecifically bound cations. In a study of Weng et al.³¹ coagulation and precipitation of a purified HA were found to depend on the Donnan potential (φ_D) resulting from the residual charge of the HA as calculated using the NICA-Donnan model. The similar results were reported by Osté et al.40 who found a linear relationship between the log DOC concentration and the φ_{D} of DOM in soil suspensions with a range in pH and Ca concentrations for eight acidic to neutral soils. These studies illustrated the importance of coagulation/dissolution in determining DOM release.

In the soil solid phase, OM exists simultaneously in different states, including particulate plant residues and decomposed/ "humified" OM that can occur in coagulated or aggregated forms and can be adsorbed to minerals.⁴¹ Organic matter

associated with minerals is known to be better protected against microbial degradation than other OM pools, and plays an important role in long-term soil organic carbon sequestration. 42 Therefore, mobilization of OM from different pools has consequences for organic carbon storage in soils. Soil properties such as pH and Ca concentration influence both adsorption and coagulation of OM. 31,40,43,44 Multivalent cations (e.g., Ca²⁺) can decrease the level of DOM in solution by promoting aggregation of OM and/or enhancing its adsorption onto negatively charged minerals via cation bridging and electrostatic effects. ^{40,43–45} An increase in pH reduces the positive charge of soil oxides and increases electrostatic repulsion between OM molecules, both of which might lead to the release of DOM via desorption or dissolution.^{6,46} According to Kaiser and Kalbitz⁴⁶ the concentration and composition of DOM are regulated by a sequence of processes including adsorption/desorption to/ from reactive minerals, precipitation/dissolution, and microbial transformation. It is, however, unclear to which extent DOM is mobilized in soil by adsorption/desorption or coagulation/ dissolution processes when pH and Ca concentration of a soil are subject to change. Quantifying the contribution of these processes to the release of DOM from soil to solution when these conditions change thus remains a challenge.

The objectives of this study are to quantify (1) the effects of pH and Ca on the concentration and composition of DOM in terms of its hydrophilic and humic components as operationally defined by a standard fractionation method (Hy, FA, HON, and HA) in a series of batch experiments, 19 (2) the solution conditions under which the release of DOM is controlled by adsorption/desorption or coagulation/dissolution processes. For the series of batch experiments, three soil samples were selected from a collection of representative Dutch agricultural topsoils.⁴⁷ The data set of our series of batch experiments was complemented with an additional data set of four soil samples from Weng et al.⁴⁸ who did similar batch experiments as those conducted here. Next, we quantified the contribution of adsorption/desorption to the release of DOM using the NOM-CD model, 25 whereas the $\varphi_{\rm D}$ of DOM calculated with the NICA-Donnan model³⁷ was used as input for the empirical model of Weng et al.³¹ to assess the importance of coagulation/dissolution in DOM release. Based on our findings, a conceptual Dual-Domain Desorption Dissolution model is proposed to describe the state and compositional change of both SOM and DOM under varying soil solution conditions. This study, to our knowledge, will be the first time quantify the different processes controlling DOM release from soil in response to changes in the pH and Ca concentration.

2. MATERIALS AND METHODS

2.1. Soil Samples. Three soil samples (referred to as soil 10, 11, and 12) were selected from a collection of representative Dutch agricultural topsoils, known as the Copernicus soil series. These soil samples were used in the series of batch experiments conducted in this study to quantify the effects of pH and Ca on the concentration and composition of DOM in solution (see Section 2.2). The data set from these batch experiments was complemented with a data set from Weng et al. Who did similar batch experiments for four other soil samples taken from the same Copernicus soil series. The four soil samples of Weng et al. are referred to as soil 3, 4, 9, and 18. An overview of the properties of all

seven soils including those of Weng et al. ⁴⁸ is given in Table S1 of the Supporting Information (SI). The seven soil samples cover a range in pH (4.5–5.6) and SOC (2.1–14%). Furthermore, they vary in the amounts of Fe- and Al(hydr)oxides, which form the major reactive surfaces controlling mineral-associated OM, and they vary as well in the phosphate (PO₄) loading of these oxides, calculated as the molar ratio between the amount of total reversibly bound PO₄ and the summed amounts of these metal-(hydr)oxides (0.06–0.22). ⁴⁹

2.2. Batch Experiments and DOM Fractionation. For the series of batch experiments with soil 10, 11, and 12 as conducted in this study, soil suspensions were prepared at a solid-to-solution ratio of 0.1 kg/L in three different background solutions (i.e., 30 mM NaCl, 2 mM CaCl₂, and 10 mM CaCl₂) across a pH range of 4-9. Furthermore, Cu was added as a probe ion to each suspension at a concentration of 5 mg/L in the form of CuCl₂ to assess the metal binding capacity of DOM. The results of the metal complexation capacity of DOM will be reported in a forthcoming publication. The pH of each suspension was adjusted to and maintained at the desired level by adding appropriate amounts of acid or base (0.1 M HCl and 0.1, 1, or 3 M KOH). The suspensions were equilibrated for 10 days by gentle horizontal shaking (35 strokes per minute) in a conditioned room at 20 °C. More details on the preparation of the soil suspensions can be found in Section S2 of the SI.

After 10 days of shaking, the final pH was measured in each soil suspension. Thereafter, the suspensions were centrifuged at 3000 rpm for 20 min, followed by 0.45 μ m membrane filtration (Aqua 30/0.45 CA Whatman) and subsequent chemical analysis. The dissolved organic carbon (DOC) concentration was measured by a segmented flow analyzer (SFA-TOC; SKALAR San++). The P-PO₄ concentration was measured colorimetrically⁵⁰ by a segmented flow analyzer (SKALAR San++). The dissolved Ca concentration was determined using ICP-AES (Thermo Scientific iCAP6500), whereas the dissolved Cu concentration was measured using either ICP-AES or HR-ICP-MS (Thermo Scientific Element 2). To gain a quantitative insight in the DOM composition, DOM was fractionated into Hy, FA, HON, and HA based on their pH-dependent hydrophilic and hydrophobic properties using the rapid batch technique of Van Zomeren and Comans.¹⁹ More analytical details of this technique can be found in Section S3 of the SI.

For the data set based on the batch experiments with soil 3, 4, 9, and 18 taken from Weng et al., 48 the same experimental approach was followed as outlined above. In their work, however, only one background solution of 10 mM CaCl₂ was used without the addition of CuCl₂. Furthermore, Weng et al. 48 performed the same chemical analyses as those performed in our batch experiments with soil 10, 11, and 12 without using the rapid batch technique 19 to fractionate DOM.

2.3. Modeling Approach. 2.3.1. Coagulation/Dissolution. In the previous study of Weng et al. in which the DOM concentration in solution was controlled by coagulation/dissolution, an empirical model was derived that describes the linear relationship between the log DOC concentration and the φ_D of DOM. In their approach, the NICA-Donnan model was used to calculate the φ_D of the DOM in solution. In the current study, we used a similar approach. This calculation was performed using two different scenarios regarding the reactivity of DOM in solution and in both scenarios, all DOM was taken into account. In scenario 1 and 2, the NICA-Donnan model

parameters of either generic FA or generic HA were used. For each scenario, the corresponding DOM concentration in solution was calculated by multiplying the DOC concentration by a factor of 2, because half of the DOM was taken to consist of carbon.⁵¹ As input for the NICA-Donnan calculations, the measured pH and dissolved Ca and Cu concentrations (Figure S1) were used. The ambient partial pressure of CO_2 (pCO_2) was set to 39.8 Pa. The dissolved Na and Cl concentrations were set equal to those of the imposed background concentrations. The dissolved K concentration was calculated from the volume of KOH added for adjusting the pH of the suspensions. The effects of Fe³⁺ and Al³⁺ on the $\varphi_{\rm D}$ of DOM were taken into account by using their activities that were calculated from the solubility of Fe(OH)₃ (log $K_{so} = -38.46$) and Al(OH)₃ (log $K_{so} = -33.96$). Depending on the scenario, the DOM was assumed to behave either as generic FA (scenario 1) or as generic HA (scenario 2). Generic NICA-Donnan model parameters for the binding of Ca, Cu, Al, and protons to HA or FA were taken from Milne et al. 52,53 For Fe binding to FA, NICA model parameters were adopted from Hiemstra and van Riemsdijk. S4 Next, the φ_D of DOM calculated with the NICA-Donnan model for the two above given scenarios was used as input for the empirical relationship derived by Weng et al.31 to explore the possible role of coagulation/dissolution in regulating DOM release.

2.3.2. Adsorption/Desorption. Organic matter and PO₄ bind competitively to the reactive surface of the soil solid phase, which is usually dominated by binding to Fe- and Al-(hydr)oxides.³⁹ Here, the amount of adsorbed NOM was derived by simulating the solid-solution distribution of PO₄ as measured in the soil batch experiments conducted in this study as well as in the study of Weng et al.⁴⁸ In the NOM-CD model, the Charge Distribution and MUlti-SIte Complexation CD-MUSIC model⁵⁵ was used to describe the reactivity and electrostatics at the surface of oxides, while the Extended Stern electrostatic model was used for the compact part of the EDL.⁵⁶ In the Extended Stern model, there are two Stern layers, the first one between the surface plane (0-plane) and first outer-electrostatic plane (1-plane) and the second between 1-plane and 2-plane (second outer-electrostatic plane).⁵⁶ In the NOM-CD model, a virtual NOM molecule (≡FeNOM) is included to represent adsorbed OM present in the Stern layers. Each virtual NOM molecule contains two carboxylic groups, which can be present in the form of an inner-sphere, an outer-sphere, or a protonated inner-sphere complex.²⁵ Ferrihydrite (Fh) was used as a proxy for the metal-(hydr)oxides in all seven soils used in the current study. Recently, Mendez et al.³⁹ showed that for a set of 19 Dutch agricultural topsoils including the seven soils used in the current study, the reactivity of the natural metal-(hydr)oxides was better described by using Fh as a proxy than by wellcrystallized goethite. The effective reactive surface area (RSA) and the amount of total reversibly bound PO₄ (R-PO₄) from Mendez et al.³⁹ (Table S1) were used as input in the NOM-CD model. In the study of Mendez et al., ³⁹ PO₄ was used as a native probe ion to derive the RSA as well as R-PO₄ for all seven soils used here, based on Fh as a proxy for the PO₄ adsorption behavior of soil oxides. Other input for the NOM-CD model calculations included measured pH and the dissolved Ca concentration in solution as well as the dissolved Na and Cl concentrations as added with the background solutions. The presence of Ca was taken into account as the adsorption of PO₄ to Fh is found to be enhanced in the

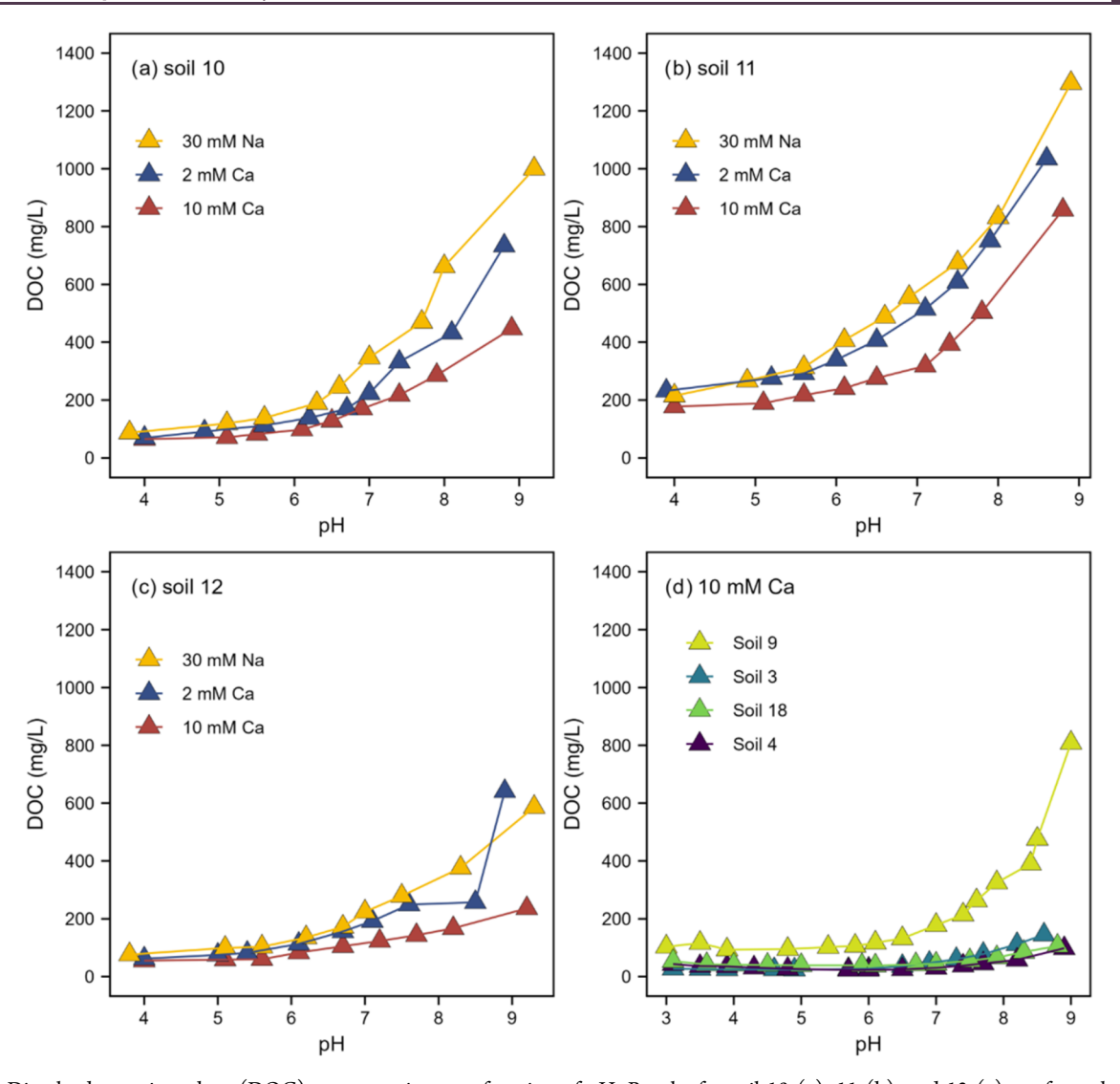


Figure 1. Dissolved organic carbon (DOC) concentration as a function of pH. Results for soil 10 (a), 11 (b), and 12 (c) are from the series of batch experiments performed in this study with three different background solutions (30 mM Na, 2 mM Ca, and 10 mM Ca). Data for soil 3, 4, 9, and 18 (d) were taken from Weng et al.⁴⁸ who used only one Ca background concentration of 10 mM.

presence of adsorbed Ca and vice versa. ⁵⁷ Consequently, the presence of Ca in our CD-NOM calculations will influence the amount of adsorbed NOM that is derived in our model calculations. The formation constants for complexation reactions in solution and reactions taking place at the oxide surface including surface species, charge distribution, and affinity constants ($\log K$) for Fh are presented in Tables S2 and S3 of the SI, respectively. The amount of adsorbed NOM was iteratively optimized to predict the dissolved PO₄ concentration as measured in solution. ³⁹

In the NOM-CD model, the amount of surface-bound OM is expressed as a surface species density in μ mol \equiv FeNOM/ m^2 , with each \equiv FeNOM molecule containing two carboxylic groups. ²⁵ In order to quantitatively compare the change in the amount of surface-bound OC with the measured change in the DOC concentration in solution, the fitted molar surface density of \equiv FeNOM (expressed as μ mol \equiv FeNOM/ m^2) was rescaled to a mass of carbon per unit mass of soil. For this conversion, generic FA was used as an analog of adsorbed NOM, because adsorbed FA is mostly present in the Stern layers, ^{27,58} similar to \equiv FeNOM in our NOM-CD model calculations. Based on the site density of carboxylic-type

groups and the carbon content of generic FA (site density = 5.88 mol/kg, 52 C content = 45%) and the RSA (m²/g soil) of the seven soil samples (Table S1), the fitted molar surface density of \equiv FeNOM was converted from μ mol \equiv FeNOM/m² to mg C/g soil.

All calculations with the NICA-Donnan model and NOM-CD model were performed using the software ECOSAT⁵⁹ and the flowchart of the two models' calculation procedures was presented in Figure S2 of the SI.

3. RESULTS AND DISCUSSION

3.1. Effects of pH and Ca on the DOC Concentration and Composition. In Figure 1, the DOC concentration is presented as a function of pH at the three background solutions for soil 10, 11, and 12 as used in the series of batch experiments performed in the current study (Figure 1a–c). The DOC concentration increased with pH and decreased with Ca background concentration. The increase in DOC concentration with pH is generally more pronounced when the pH is above ~6.5. Likewise, the effect of Ca background concentration is more pronounced at a relatively high pH. For

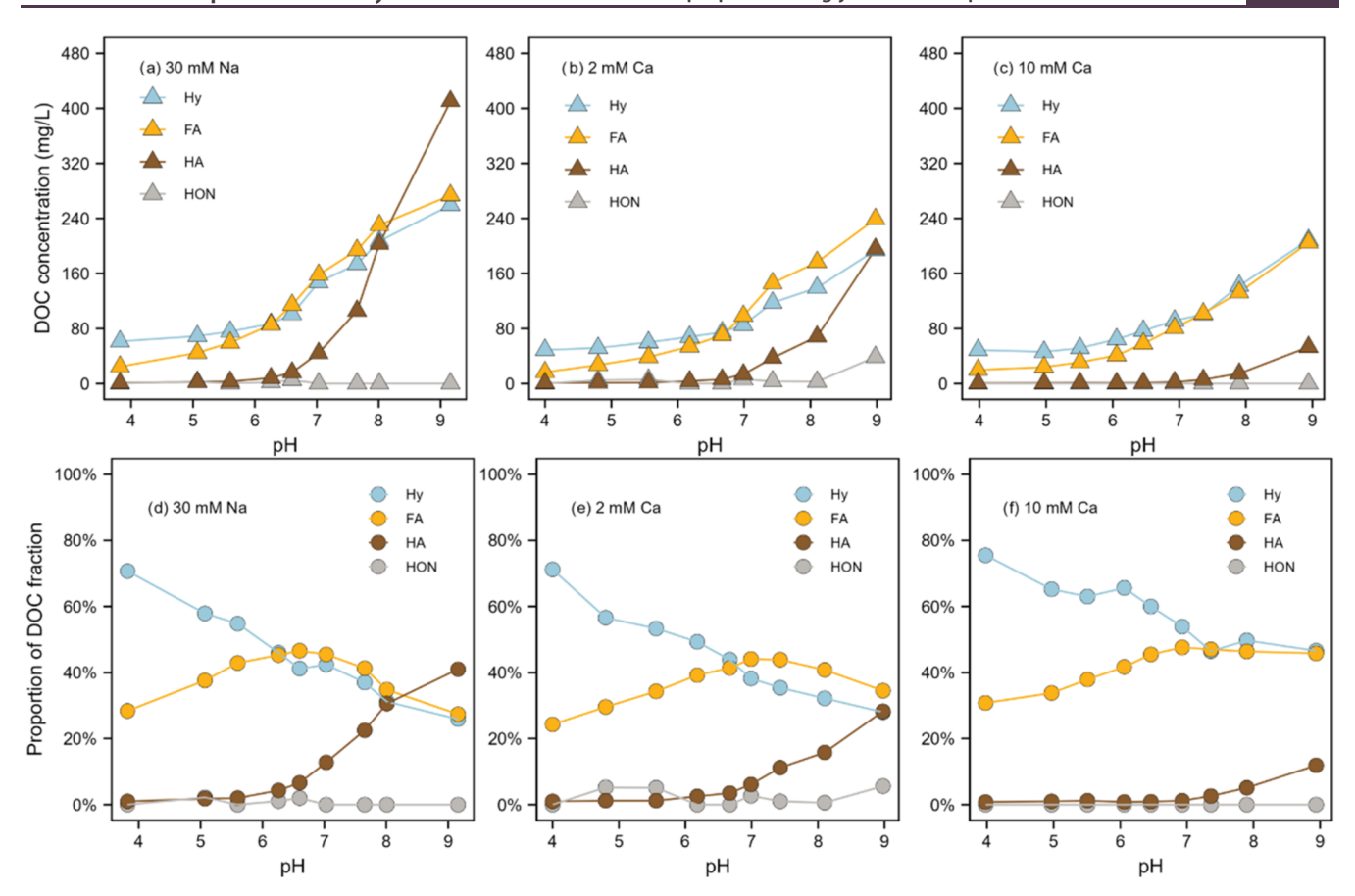


Figure 2. Concentrations (a-c) and proportions (d-f) of the Hy, FA, HON, and HA fractions constituting dissolved organic carbon (DOC) as a function of pH at the three different background concentration (30 mM Na, 2 mM Ca, and 10 mM Ca) for soil 10. The results of soil 11 and 12 are present in Figure S4 of the SI.

the same pH, an increase in Ca background concentration from 2 to 10 mM led to a greater decrease in the DOC concentration than an increase from 0 (30 mM Na) to 2 mM Ca. Our findings are consistent with results from previous studies reporting an increase in the DOC concentration in solution with an increase in pH^{60-62} as well as a decrease in DOC concentration with an increase in the Ca concentration. 40,45 The amount of DOC expressed as a percentage of the SOC content ranged from 0.8 to 24.1%, depending on the pH and Ca background concentration (Figure S3). For soil 3, 4, 9, and 18 taken from Weng et al., 48 only one Ca background concentration of 10 mM was used, which is the same as the highest Ca background concentration used in our series of batch experiments with soil 10, 11, and 12. The results of Weng et al.⁴⁸ are largely comparable to those of the current study, although the DOC concentration for soil 4 and 18 did not show a gradual increase with pH in the pH range from 3 to 6 (Figure 1).

To investigate the effects of pH and Ca on the DOM composition, DOM of soil 10, 11, and 12 was fractionated into Hy, FA, HON, and HA using the rapid batch technique of Van Zomeren and Comans.¹⁹ The concentration and contribution of each fraction to the total DOC concentration are shown in Figure 2 (soil 10) and Figure S4 (soil 11 and 12). Similar to the DOC concentration (Figure 1), the concentrations of Hy, FA, and HA increased with pH for the three background solutions (Figures 2 and S4). However, the concentration of the HON fraction, which is the lowest of all fractions considered in the fractionation scheme used here, hardly

changed with pH. For all three soils, the concentration of the HA fraction increased more strongly with pH than the Hy and FA fractions in the presence of the 0 and 2 mM Ca background concentrations. You et al. 62 found a similar result showing that the higher molecular weight OM, especially HA, was increasingly released from soil to solution at higher pH. The higher Ca background concentration of 10 mM decreased the concentrations of the Hy and FA fractions for the three soils only slightly, whereas it strongly decreased the concentration of the HA fraction, particularly above neutral pH. For the 10 mM Ca background concentration, the HA fraction contributed on average only 4% to the total DOC concentration across the entire pH range for the three soils. For comparison, the HA fraction measured for the 0 mM Ca background concentration became the dominant component of total DOC at pH \sim 9 for soil 10, 11, and 12. In the study of Römkens and Dolfing,⁴⁵ Ca addition was suggested to induce preferential coagulation and subsequent precipitation of the HA fraction, which may explain why the HA concentration decreased the most with an increase in the Ca background concentration.

At the lowest pH used in our series of batch experiments, DOC is dominated by the Hy fraction, contributing 76, 67, and 74% to total DOC for soil 10, 11, and 12 respectively (Figures 2 and S4). The contribution of the FA fraction to total DOC at the lowest pH amounts to 31, 33, and 27% for soil 10, 11, and 12, respectively. The contribution of the HA fraction is negligible at the lowest pH, while the contribution of the HON fraction is below 2.6% across the entire pH range for the three background concentrations. The Hy fraction generally contains

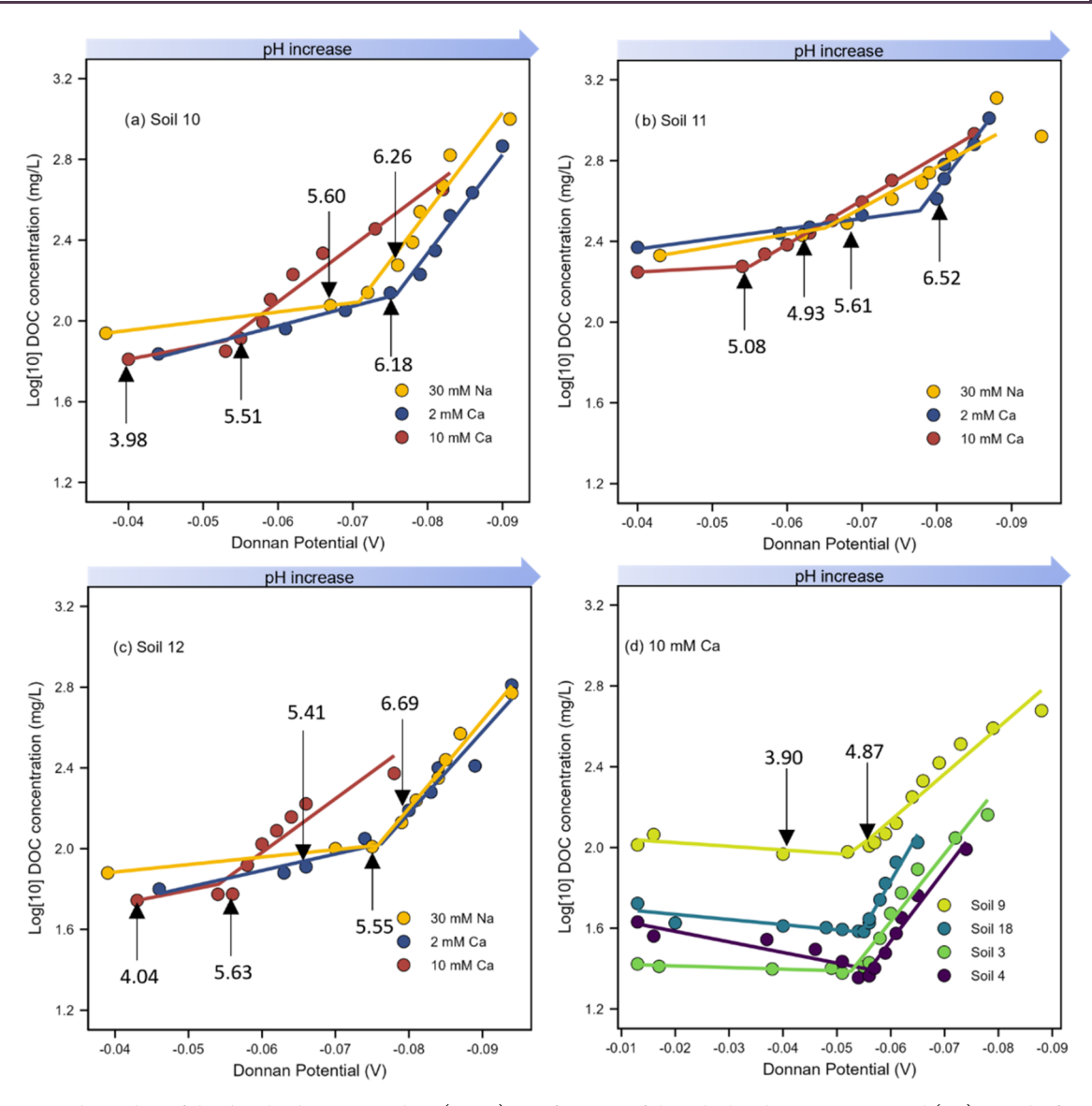


Figure 3. Base-10 logarithm of the dissolved organic carbon (DOC) as a function of the calculated Donnan potential (φ_D). Results for soil 10 (a), 11 (b), and 12 (c) are from the series of batch experiments performed in this study with three different background solutions (30 mM Na, 2 mM Ca, and 10 mM Ca). Results presented in (d) are for soil 3, 4, 9, and 18 of Weng et al. who used only one Ca background concentration of 10 mM. Please note: φ_D plotted on the x-axis becomes more negative from the left to the right, whereas pH increases from the left to the right. Furthermore, φ_D in (d) starts at a less negative value than in (a–c), because the lowest pH in the study of Weng et al. whereas in our series of batch experiments the lowest pH was ~4. The φ_D was calculated with the NICA-Donnan model using scenario 2 in which NICA-Donnan model parameters for generic humic acid (HA) were used. The solid lines represent the fitted broken-line models. The fitted model coefficients can be found in Table S4 of the SI. The black arrow with a number indicates the pH value for a specific data point.

low molecular weight organic solutes such as sugars and small organic acids, ²⁹ which tend to dissolve easily at both low and high pH. For all three soils, the dominance of the Hy fraction at low pH diminished when pH increased to \sim 6, \sim 7, and \sim 7.5 for the 0, 2, and 10 mM Ca background concentrations, respectively. With a further increase in pH, the absolute Hy and FA concentrations and their contributions to total DOC are rather similar. The contribution of Hy fraction to total DOC decreased with pH over the entire pH range for the three background concentrations for all three soils. However, the contribution of the FA fraction first increased with pH to pH \sim 7, which was then followed by a decrease when pH further increased, especially for the 0 and 2 mM Ca background concentrations. Hence, the FA contribution to total DOC showed a maximum when the pH was close to near-neutral

pH. The contribution of the HA fraction to total DOC increased across the entire pH range for all three background concentrations. However, the contribution of the HA fraction to total DOC was nevertheless lower than the contributions of the Hy and FA fractions with the exception of pH 8–9 for the 0 and 2 mM Ca background concentrations where the HA fraction dominated the composition of the total DOC in solution.

3.2. Effects of pH and Ca on the Donnan Potential of DOM. Formation of OM coagulates or supramolecules depends on forces of interparticle interactions, including both attractive forces (e.g., hydrophobic interaction, H-bonding, and cation-bridging) and repulsive forces (e.g., electrostatic repulsion). Soil organic matter is overall negatively charged, where a more negative charge and potential implies a

stronger electrostatic repulsion between its constituent molecular components, which, in turn, lowers its tendency to form coagulates and leads to a higher solubility. Similar to Weng et al. 31 and Osté et al. 40 we used the NICA-Donnan model to calculate the $\varphi_{\rm D}$ of DOM, based on the two scenarios with different assumptions for the reactivity of DOM in terms of FA and HA (see Section 3.1). The calculated $\varphi_{\rm D}$ as a function of pH and Ca background concentration was nearly the same for both scenarios (Figure S5). For all three soils, the φ_{D} of DOM at all Ca background concentrations became more negative with pH. For the same pH, the ϕ_{D} was more negative at a lower Ca background concentration. NICA-Donnan model calculations based on scenario 1 where 100% of DOM was taken as FA yielded a slightly more negative φ_D than calculations using scenario 2 with 100% of DOM as HA. The results of these calculations are consistent with the higher site density of carboxylic-type groups on FA than on HA, leading to a higher negative charge and $\varphi_{\rm D}$ of FA at a given pH and Ca background concentration.

In Figure 3, the log DOC concentration measured in solution is presented as a function of the φ_D , calculated using scenario 2 with NICA-Donnan parameters for generic HA. Plotting the log DOC concentration against the φ_{D} calculated using scenario 1 yields similar trends as those presented in Figure 3, because the $\varphi_{\rm D}$ differs only slightly between the two scenarios (Figure S5). The log DOC concentration at each Ca background concentration increased when ϕ_{D} became more negative for all seven soils considered in this study. The relationships between the log DOC concentration and φ_{D} in Figure 3 can be divided into two linear sections on either side of a so-called change point. The slope of the linear relationship in the section above the change point (high pH range) is steeper than the slope in the section below the change point (low pH range). Such data can be fitted with a broken-line model with two linear relationships having distinct slopes and intercepts, which are connected at this change point. Based on this model, a good linear relationship was found between the log DOC concentration and ϕ_{D} below and above the change point for each Ca background concentration for all seven soils used in this study (Table S4). For the 0 and 2 mM Ca background concentrations, a change point was observed at a φ_D of \sim -0.075 V (corresponding to a pH of \sim 5.5-6.5), whereas a change point for the 10 mM Ca background concentration occurred at a φ_D of \sim -0.055 V (corresponding to a pH of \sim 5) (Figure 3 and Table S4). The less negative φ_D of the change point fitted for the 10 mM Ca background concentration may be due to a stronger effect of Ca in promoting OM adsorption to soil than for OM coagulation, which may explain why dissolution of OM starts to become the dominant process at a less negative φ_{D} and a lower pH for the Ca background concentration of 10 mM. The similar ϕ_{D} values of the change points for the 0 and 2 mM Ca background solutions are consistent with the dissolved Ca concentrations that were measured in the presence of these backgrounds. Although different background solutions of 30 mM Na and 2 mM Ca were used to prepare the soil suspensions, the measured Ca concentrations after equilibration with the soils were nearly the same (Figure S1). This can be explained by Ca desorption from the soil solid phase to solution for the 30 mM Na background solution and a combination of Ca desorption at lower pH and Ca adsorption at higher pH for the 2 mM Ca background solution. For the 10 mM Ca background solution,

the measured Ca concentration after equilibration was substantially higher than the Ca concentrations of the other two background solutions, except for the highest pH (Figure S1). The results of the broken-line model suggest the existence of two different mechanisms that dominate the release of DOM from soil to solution below and above the change point in φ_D , corresponding to a pH of ~5.5–6.5 for the 0 and 2 mM Ca background concentrations and a pH of ~5 for the 10 mM Ca background concentration (Figure 3). When the pH is below this change point, adsorption/desorption may dominate DOM release, which is discussed in Section 3.3. When the pH is above this change point, the greater increase in the log DOC concentration with a more negative φ_D can be explained by a stronger electrostatic repulsion between the molecular components constituting SOM, which leads to a higher solubility of OM. This mechanism of OM precipitation/ dissolution will be discussed in Section 3.4.

Osté et al.40 found strong linear relationships between the $\log {
m DOC}$ concentration and $\varphi_{
m D}$ in soil suspensions with a range in pH and Ca concentrations prepared for eight acidic to neutral soils. In contrast to our observations (Figure 3 and Table S4), Osté et al. 40 did not observe a change point in their relationships. This may be explained by a limited range in pH for their series of soil suspensions as they added only base to their suspensions, 40 whereas both acid and base were added to the suspensions of all seven soils considered in our study. Furthermore, the slopes and intercepts of the linear relationships between the log DOC concentration and φ_D derived by Osté et al.⁴⁰ differed greatly for their eight soils. The same was found for all seven soils considered in the current study (Figure 3 and Table S4). However, the reason behind the observed variation in the slopes of the linear relationships derived by Osté et al.40 remained speculative so far. The possible explanation can be found in Section 11 of the SI. Irrespective of the steepness of the slope, the change point in the relationship between log DOC and φ_D points to the existence of two different mechanisms dominating the release of DOM below and above pH ~5.5-6.5 for the 0 and 2 mM Ca background concentrations and pH ~5 for the 10 mM Ca background concentration (Figure 3), which we will further investigate in the following Section 3.3.

3.3. Effects of pH and Ca on Organic Matter **Adsorption and Desorption.** To further investigate the mechanisms controlling the release of DOM from soil to solution as a function of pH and Ca concentration, the amount of adsorbed OM was calculated with the NOM-CD model. The amount of OM adsorbed closely to the surface (in the Stern layers) of metal-(hydr)oxides was derived as a fitting parameter by predicting the measured dissolved PO₄ concentration in solution using R-PO₄ and RSA (Table S1) as model input. Subsequently, the change in the amount of adsorbed OM as calculated by the NOM-CD model with pH was related to the change in the DOC concentration measured in solution for each of the three background solutions. In Figure S7, the dissolved P-PO₄ concentration of soil 10, 11, and 12 as a function of pH at the three different background solutions is presented. The P-PO₄ concentration of these soils ranges from 0.01 to 11.1 mg P/L (0.32–358 μ M). The effects of pH and Ca on the PO₄ concentration are discussed in Section S12 of the SI. For soil 10, most of the measured P-PO₄ concentrations are close to the detection limit (i.e., 0.02 mg P/ L), especially when pH < 7, which can be largely explained by the low PO₄ loading of this soil (Table S1).

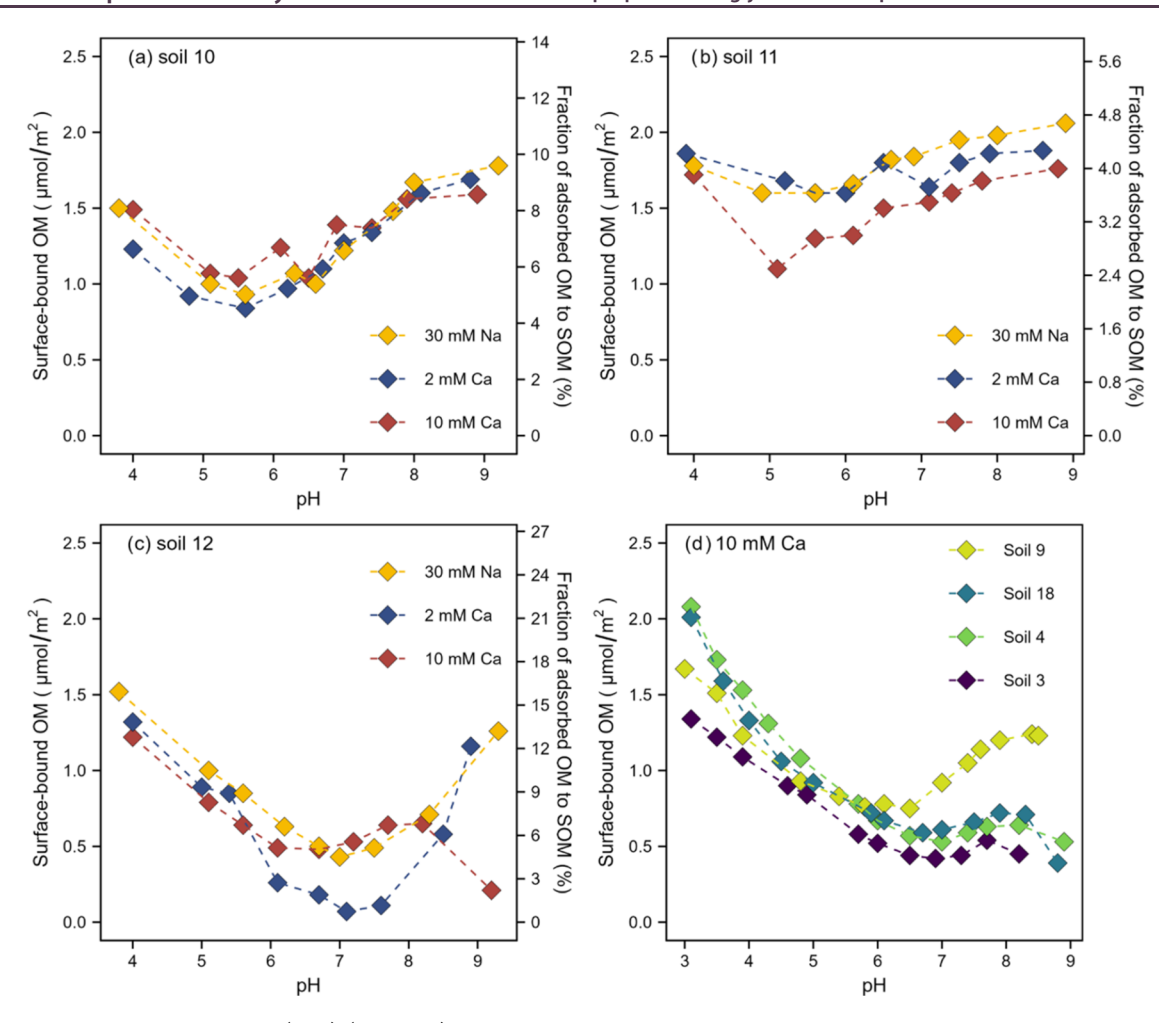


Figure 4. Surface-bound organic matter (OM) (left y-axis) as a function of pH calculated with the NOM-CD model. Organic matter adsorption for soil 10 (a), 11 (b), and 12 (c) was calculated at three different background solutions used in the current study (30 mM Na, 2 mM Ca, and 10 mM Ca), whereas OM adsorption for soil 3, 4, 9, and 18 (d) of Weng et al. was only calculated for a background concentration of 10 mM Ca. In the NOM-CD model calculations, ferrihydrite (Fh) was used as a reference soil oxide to predict the measured PO₄ concentration in solution with the soil-specific effective reactive surface area (RSA) and reversibly bound PO₄ concentration (R-PO₄) from Mendez et al. (Table S1) as model input. On the right y-axis of (a-c), the amount of adsorbed OM is expressed as a percentage of SOM. The fraction of adsorbed OM to SOM for soil 3, 4, 9, 18 can be found in Figure S9.

The modeled amount of surface-bound OM as a function of pH is shown in Figure 4 for all seven soils considered in this study, revealing a "V"-shaped pattern. Surface-bound OM first decreases when pH increases from acidic to near-neutral pH conditions, followed by an increase when pH increases to alkaline pH conditions, resulting in a minimum in surfacebound OM at pH ~5 to 7. This minimum in surface-bound OM is found at a relatively low pH of ~5-6 for soils with relatively high SOC content (soil 10 and 11; Table S1), but shifts toward a higher pH of ~7 for the other soils exhibiting a lower SOC content. When 10 mM Ca was used as a background solution, a drop in surface-bound OM was observed at pH ~ 9 for the soils with a relatively low SOC content (soil 12, 3, 4, and 18). These soils have a relatively high PO₄ loading (Table S1), which may have led to the precipitation of calcium phosphate minerals.⁴⁸ Consequently, this may have led to modeling artifacts when deriving surfacebound OM due to the lack of a direct relation between the adsorption of OM on the surface of soil oxides and the concentration of PO₄ in solution.

When the pH increases from acidic (\sim 3–4) to less acidic to neutral pH conditions (\sim 5–7), the amount of surface-bound

OM decreases with pH. As a result, surface-bound OM desorbs from the reactive surface of soil oxides, thus releasing DOC to the solution. However, surface-bound OM increases again with pH above a pH of $\sim 5-7$ until a pH of ~ 9 . This may be attributed to the fact that some DOM fractions released by the dissolution process may be readsorbed onto soil minerals. Therefore, desorption of surface-bound OM cannot explain the increase in the DOC concentration in solution in the high pH range (Figure 1). Instead, dissolution of coagulated and precipitated OM is more likely to control DOC release in this pH range. This interpretation is further strengthened by the observed change point in the relationship between the measured log DOC concentration in solution and $\varphi_{\rm D}$ (Figure 3 and Table S4) above which the log DOC concentration increased more strongly with a more negative φ_D (Figure 3). Hence, this change point may indicate a transition from a domain where adsorption/desorption dominates the release of DOM to a domain where coagulation/dissolution becomes more important. In Sections 3.4 and 3.5, we will quantitatively analyze the contributions of these two mechanisms to the change in the measured DOC concentration in solution as a function of pH and Ca background concentration.

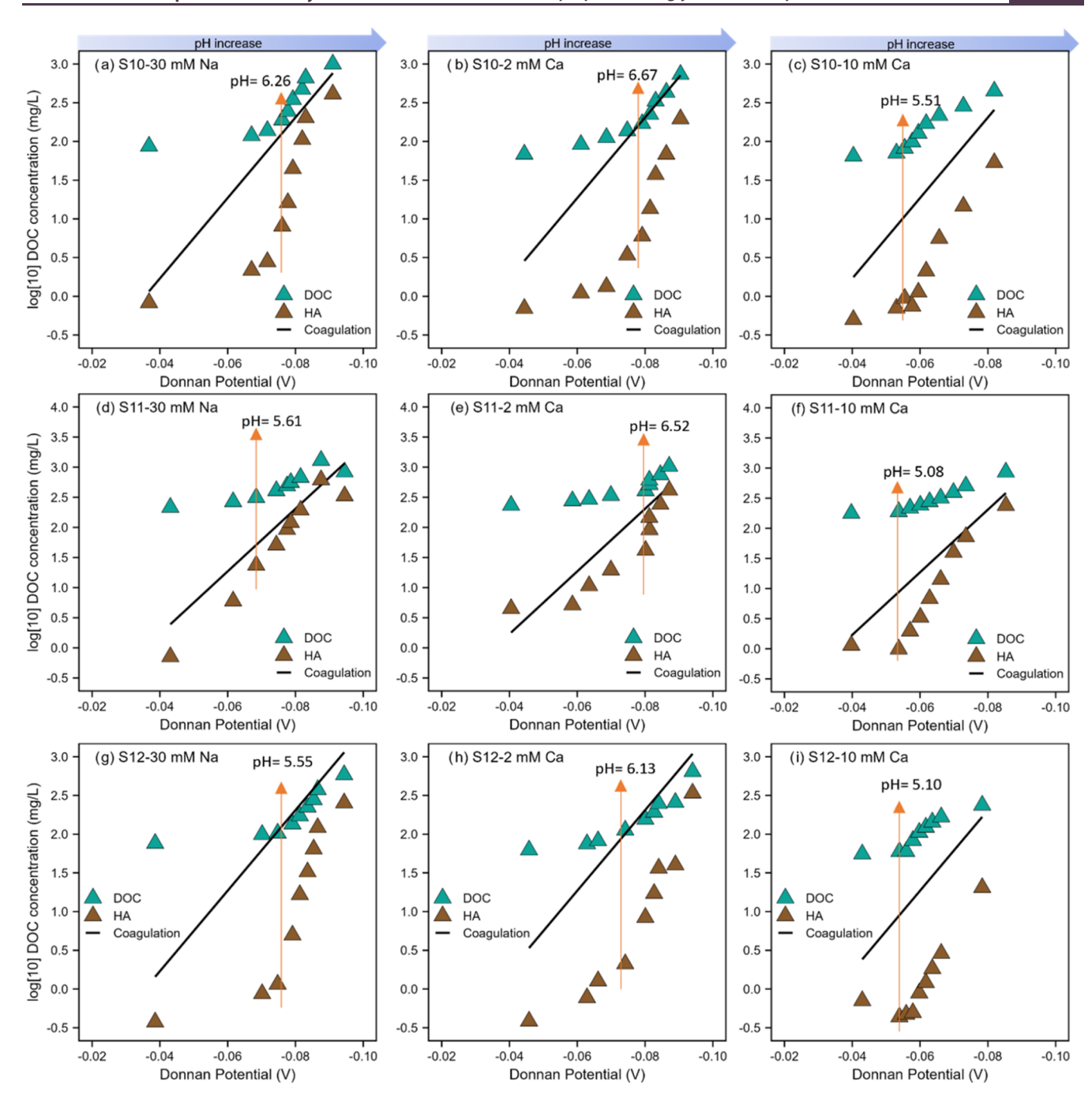


Figure 5. Base-10 logarithm of the concentrations of total dissolved organic carbon (DOC) and humic acid (HA) as a function of the Donnan potential (φ_D) calculated with the NICA-Donnan model for soil 10 (a-c), 11 (d-f), and 12 (g-i) at three different background solutions (30 mM Na, 2 mM Ca, and 10 mM Ca). The φ_D was calculated based on using NICA-Donnan parameters of generic HA for proton and cation binding. ^{52,53} The black line indicates the DOC concentration calculated using the empirical relationship derived based on the coagulation/dissolution behavior of purified HA (eq 1). ³¹ The orange arrow with the number indicates the pH value of a specific data point near the change point in φ_D (Figure 3).

3.4. Coagulation/Dissolution Controlled DOM Release. Based on the $\varphi_{\rm D}$ of DOM calculated with the NICA-Donnan model, an empirical equation (eq 1) was derived by Weng et al.³¹ from batch experiments to quantify the coagulation/dissolution behavior of a purified HA

$$\log_{10}(DOC) = -52.0\varphi_{D} - 1.85 \tag{1}$$

where the DOC concentration is expressed in mg C/L and the $\varphi_{\rm D}$ is given in V. The total DOC and HA concentrations of soil 10, 11, and 12 as measured in our series of batch experiments

are compared with the log DOC concentration calculated from $\varphi_{\rm D}$ by using eq 1 in Figure 5. The $\varphi_{\rm D}$ used here was calculated with the NICA-Donnan model based on scenario 2 in which 100% of the measured DOC concentration was assumed to be HA (Figure 5). The same comparison was made for soil 3, 4, 9, and 18 from Weng et al. (Figure S8). For these soils, however, no HA fractionation data are available. For this reason, the log DOC concentration calculated using eq 1 was only compared with the measured total DOC concentration for these soils. For soil 10, 11, and 12, the measured total DOC concentrations above the change point in $\varphi_{\rm D}$ (Figure 3 and

Table S4) corresponding to the high pH range agree reasonably well with those predicted by eq 1 (Figure 5), except for the 10 mM Ca background concentration. For this background concentration, the measured total DOC concentrations are higher than those predicted using eq 1. In addition to the HA fraction, the Hy and FA fractions also significantly contribute to the total DOC concentration (Figures 2 and S4). For the high pH range and the 10 mM Ca background concentration of soil 10, 11, and 12, the contributions of the Hy and FA fractions to the total DOC concentration are larger than the contribution of the HA fraction, except for soil 11 at the highest pH of ~9 where the contributions of the Hy, FA, and HA fractions to total DOC are quite the same.

It has been proposed that different OM fractions varying in molecular mass and solubility may form larger OM associations of supramolecular structures. 32,33 It is very likely that supramolecular aggregates become more dispersed and release DOM at high pH as a result of an increase in electrostatic repulsion, explaining why the total DOC increases when the $\varphi_{\rm D}$ becomes more negative (Figure 3). Disintegration of supramolecular aggregates can subsequently result in the release of different smaller components, which may be operationally identified as HA, FA, or Hy based on their pHdependent solubility and hydrophobic properties.¹⁹ This explains why the concentrations of all DOM fractions, not only that of HA, but also those of Hy and FA, increase in the high pH range (Figures 2 and S4). Van Zomeren and Comans¹⁹ have shown that at low DOC concentrations in solution, a significant fraction of DOM prepared from purified HA can be operationally identified as FA and Hy, confirming that disintegration of HA (supra)molecules can occur. The increase of Ca background concentration suppresses especially the release of HA-like OM fractions from supramolecular structures.⁶³ This explains why the contribution of the HA fraction to total DOC decreases with an increase in the Ca background concentration in Figures 2 and 5. At the 0 and 2 mM Ca background concentrations, DOM is dominated by HA at high pH and the measured total DOC concentration agrees reasonably with DOC concentration predicted by eq 1 in this pH range. However, at the Ca background concentration of 10 mM, DOM largely consists of Hy and FA (Figures 2 and S4), and the DOC concentration predicted with eq 1 is lower than the measured total DOC concentration but higher than the measured HA concentration for all three soils (Figure 5). The comparison of the measured total DOC concentration with the DOC concentration as predicted by using eq 1 for soil 3, 4, 9, and 18 from Weng et al. 48 (Figure S8) yields the same observations as for soil 10, 11, and 12 (Figure 5). Hence, coagulation/dissolution is likely the principal mechanism governing the release of DOC in the high pH range when the pH is $>\sim$ 5-6.5. However, eq 1 was derived based on coagulation batch experiments using one single purified HA isolated from forest floor material.³¹ Purified humic acids isolated from different sources may differ in properties such as the density of carboxylic- and phenolictype groups and the affinities of cations to bind to these functional groups. 52,53 Consequently, the $\varphi_{\rm D}$ of the DOM released to solution for our soils at any given DOC concentration may differ from the φ_{D} of the purified HA of Weng et al.,31 thus possibly causing a deviation of our experimental HA data for soil 10, 11, and 12 from the log DOC concentration as calculated with eq 1.

In the low pH range, the DOC composition is dominated by the Hy and FA fractions, which are more soluble than HA under these pH conditions (Figures 2 and S4). For this low pH range, adsorption/desorption processes are, therefore, more likely to control DOM release, which we will quantitatively analyze in Section 3.5.

3.5. Adsorption/Desorption Controlled DOM Release. The amount of surface-bound OM in the Stern layers was first compared to SOM (Figures 4 and S9). The ratio of surfacebound OM to SOM ranges from 4.5 to 9.6% for soil 11, 2.5-4.7% for soil 10, 0.7-15.9% for soil 12, and 4.0-31.3% for soil 3, 4, 9, and 18. For the 10 mM Ca background concentration at pH \sim 4, a higher surface-bound OM to SOM ratio (>13%) was observed in soils 3, 4, 12, and 18, which have a relatively low SOC content (<3.7%; Table S1). In contrast, a lower surface-bound OM to SOM ratio (<11%) was found in soils 9, 10, and 11, which have a relatively high SOC content (>5.0%; Table S1). However, surface-bound OM derived using the NOM-CD model is an estimate of the amount of OM present in the Stern layers, which have a thickness of about 0.8 nm, 56 and are close to the surface of metal-(hydr)oxide minerals. In soil, normally more than half of SOM is associated with soil minerals, while less than half is composed of particulate organic matter (plant residues).⁶⁴ Clearly, the contribution of the amount of surface-bound OM to SOM as found in our study is lower than what is usually found for mineral-associated OM, because OM bound at a greater distance from the surface in the diffuse layer (DL) is not included in the amount of surface-bound OM.

Since the NOM-CD model optimizes the amount of adsorbed OC by predicting the dissolved PO₄ concentration measured in solution, it cannot directly predict the DOC concentration in equilibrium with adsorbed OC. However, we can compare the change in surface-bound OC ($\Delta \equiv FeNOM$) with the change in the measured DOC concentration (ΔDOC) when the pH changes for the three Ca background concentrations. To do this, the lowest pH of ~4 as used in our series of batch experiments was taken as a reference. The $\Delta \equiv$ FeNOM at each discrete pH in the range between pH ~ 4 and the pH where surface-bound OM began to increase with pH (Figure 4), where adsorption/desorption is assumed to dominate the release of DOM, was calculated by subtracting the amount surface-bound OC from the amount of surfacebound OC at pH ~ 4 to quantify the amount of OC released by desorption. Similarly, Δ DOC was calculated by subtracting the DOC concentration measured at pH ~ 4 from the measured DOC concentration at each discrete pH in the range until the pH was reached at which surface-bound OM increased again (Figure 4). The quantitative comparison between ∆≡FeNOM and ∆DOC for soil 10 and 12 is presented in Figure 6. The results of soil 11 are not included because coagulation/dissolution processes, likely resulting from by its higher SOC content (Table S1), appear to control DOM release over a wider pH range, potentially starting already at pH \sim 5 (Figure 4). Although only a limited number of data points are available for this analysis, the results show a positive linear relationship between $\Delta \equiv \text{FeNOM}$ and ΔDOC in soil 10 and 12. Hence, the change in the DOC concentration in the low pH range likely originates from adsorption/desorption of surface-bound OM. However, the Δ ≡FeNOM is on average 5.7, 6.4, and 23.5 times larger than ΔDOC for the 0, 2, and 10 mM Ca background solutions, respectively (Figure 6). This can be explained by a change in

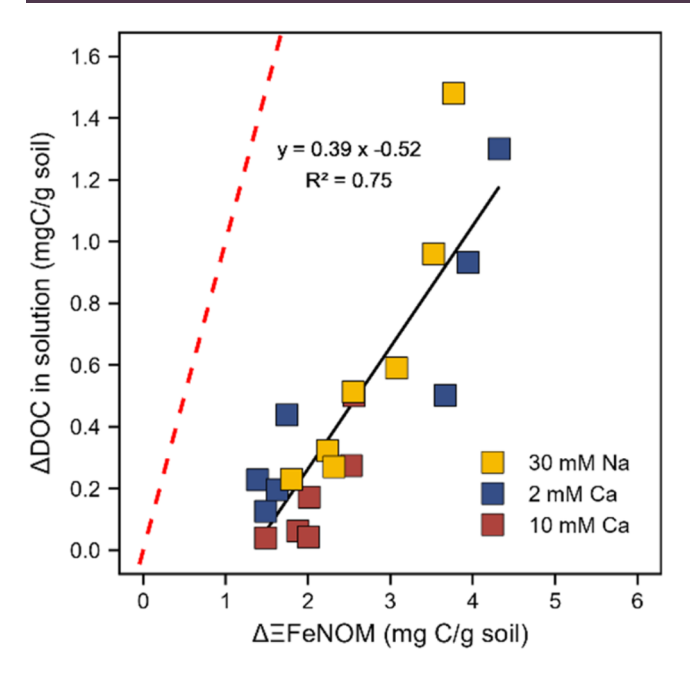


Figure 6. Relation between the change in modeled surface-bound organic carbon ($\Delta \equiv \text{FeNOM}$) and change in measured dissolved organic carbon concentration (ΔDOC) in solution for soil 10 and 12 at three different background solutions (30 mM Na, 2 mM Ca, and 10 mM Ca). Both $\Delta \equiv \text{FeNOM}$ and ΔDOC are expressed in the same unit to facilitate a quantitative comparison. The $\Delta \equiv \text{FeNOM}$ at different pH values in the range between reference pH \sim 4 and the pH where surface-bound OM began to increase with pH (Figure 4) was calculated by subtracting the amount of surface-bound OC at a certain pH from that at the reference pH \sim 4. Likewise, the ΔDOC was quantified by calculating the increase in the measured DOC concentration at each pH relative to the lowest pH \sim 4. The solid line is the fitted linear regression model, whereas the dashed red line is the 1:1 line.

the molecular conformation of the adsorbed OM. As pH increases, the conformation of adsorbed OM may change from flat on the surface of metal-(hydr)oxides to a more sphericallike conformation, ⁶⁵ extruding out of the compact Stern layers but still remaining in the DL. ^{25,27} Consequently, a part of the $\Delta \equiv$ FeNOM is not released to solution, but is retained in the DL, explaining why $\Delta \equiv$ FeNOM is higher than Δ DOC. Using a mass density for surface-bound OM of $1250 \times 10^3 \text{ g/m}^3$ combined with the RSA (Table S1),³⁹ the OM that was desorbed from the surface of metal-(hydr)oxides but was retained in the DL can contribute to a flat thickness of 0.01-0.4 nm for soil 10, 11, and 12 for the three Ca background concentrations, which is clearly less than the thickness (~0.8 nm) of the Stern layers. On average, the largest difference between the ∆≡FeNOM and ∆DOC was observed in 10 mM Ca background solution, which can be explained in two different ways. One explanation is that Ca bridging promotes the adsorption of desorbed surface-bound OC in the DL as mentioned above. 42,66 The other is that OM desorbed from the surface of soil oxides coagulates with Ca, thereby reducing the DOC concentration through precipitation.⁴⁵

For soil 3, 4, 9, and 18 from Weng et al.,⁴⁸ the pH was acidified to a lower pH level (\sim 3) compared to soil 10, 11, and 12 used in the series of batch experiments performed in the current study where pH was acidified to a pH of \sim 4. For this lower pH of \sim 3, another factor that needs to be considered is the dissolution of Fe- and Al-(hydr)oxides. A detailed

calculation and interpretation of the contribution of the dissolution of metal-(hydr)oxides and the release of associated OM to the change in the measured DOC concentration for soil 3, 4, 9, and 18 is provided in Section S16 of the SI. For this reason, the correlation between ∆≡FeNOM and ∆DOC in soil 3, 4, 9, and 18 was not included in Figure 6. For soil 10, 11, and 12, however, the dissolution of metal-(hydr)oxides has a minimal influence on the DOC concentration changes for two reasons: (1) the lowest pH level in our series of batch experiments was pH ~ 4 for which the dissolution of metal-(hydr)oxides is not yet important, as we inferred from the very low concentrations of Al and Fe that were released for soil 3, 4, 9, and 18 at this pH (Weng et al., 48 Figure S10) and (2) the measured DOC concentration of soil 10, 11, and 12 at pH \sim 4 varies between 55 and 177 mg/L, which is often higher than the DOC concentration of soil 3, 4, 9, and 18 at this pH as it varies between 25 and 93 mg/L. Hence, this would render the contribution of DOC release from partial dissolution of metal-(hydr)oxides negligible at pH ~4, even if it would occur.

4. SYNTHESIS

In this study, we investigated the mechanisms controlling DOM release at varying solution conditions of pH and Ca background concentration. Data collected from this study, together with the data from a previous study of Weng et al., were interpreted with two surface complexation models: the NICA-Donnan model³⁷ and the NOM-CD model.²⁵ In general, the DOC concentration increases as pH increases, with a more pronounced effect when pH > \sim 6.5, but decreases with an increase in the Ca background concentration. Although the concentrations of the Hy, FA, and HA fractions increase with pH, their relative contribution to total DOC changes differently. The Hy fraction is the dominant fraction at low pH (\sim 4-6), but its contribution to total DOC decreases when pH increases. The contribution of the HA fraction to total DOC increases with pH and becomes the major fraction at high pH (\sim 8–9) for the Ca background solutions of 0 and 2 mM. Regarding the FA fraction, its contribution to the total DOC concentration reaches a maximum at near-neutral pH $(\sim 6.5-7)$. For the set of agricultural topsoils investigated in this study, changes in the DOC concentration between pH $\sim 3-4$ to $\sim 5-6.5$ are mainly regulated by adsorption/ desorption of mineral-bound OM, whereas changes in the DOC concentration when the pH is above \sim 5–6.5 are likely to be controlled by coagulation/dissolution of OM. Calcium promotes both the coagulation of OM and the adsorption of OM to soil metal-(hydr)oxides. For a soil with a high Ca background concentration, the coagulation/dissolution process dominates the release of DOM over a wider range in pH.

Based on the above-described findings, we propose here a "Dual-Domain Desorption Dissolution (4D)" conceptual model (Figure 7) to illustrate the physical-chemical processes governing DOM release from soil to solution as a function of pH and Ca (and likely other multivalent cations). In the soil solid phase, OM exists as mineral-adsorbed OM and OM in (supramolecular) aggregates. Adsorbed OM possibly mainly consists of highly charged and relatively small-sized OM fractions (i.e., FA and Hy-like OM) and to a lesser extent of less charged, larger sized, and more hydrophobic OM fractions (i.e., HA-like OM), whereas supramolecular aggregates are likely more dominated by HA-like OM fractions.³³ From acidic to near-neutral pH conditions, desorption predominantly controls changes in the DOC concentration in solution when

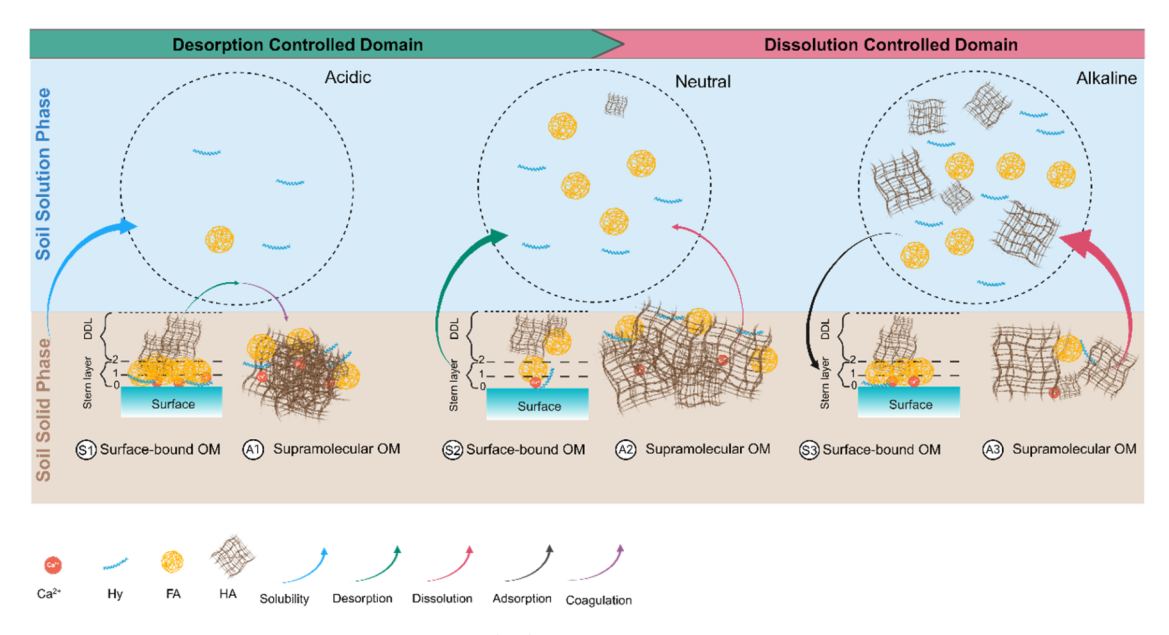


Figure 7. Conceptual Dual-Domain Desorption Dissolution (4D) model. The physical-chemical processes regulating dissolved organic matter (DOM) release from soil to solution is classified into a "Desorption Controlled Domain" (from acidic to near-neutral pH) and a "Dissolution Controlled Domain" (from near-neutral to alkaline pH). DOM in soil can be fractionated based on their relative solubility into hydrophilic acids (Hy), fulvic acids (FA), and humic acids (HA). Both Hy, FA, and HA can bind to soil minerals and be present in the Stern layers as well as in the diffuse layer (DL). Different soil organic matter (SOM) fractions varying in molecular mass and solubility may associate, forming heteroaggregates or supramolecular structure through hydrophobic interactions, cation bridges, and H-bonds. 32,33 Disintegration of the supramolecular aggregates results in release of different components, which can be operationally identified as HA, FA, or Hy based on their pH-dependent solubility and hydrophobic properties. Multivalent cations (e.g., Ca) can promote both the adsorption and coagulation of OM. The thickness of the arrow represents the quantitative contribution of each process to the DOC concentration in solution.

pH and/or Ca concentration vary (Desorption Controlled Domain). At acidic pH, DOM in solution is largely composed of Hy and FA owing to their high solubility, while the less soluble HA coagulated as (supramolecular) aggregates remain largely insoluble at this pH. When the pH increases from acidic to near-neutral pH conditions, the mineral oxide surface becomes less attractive for adsorption of OM due to deprotonation. Mineral-bound OM desorbs from the oxide surface, releasing mainly Hy and FA to the solution. However, only a part of the OM that has desorbed from the oxide surface actually ends up in solution, as desorbed OM may to some extent remain in the DL or the desorbed OM may coagulate together with existing (supramolecular) aggregates (i.e., Ca bridging). As pH increases, OM (supramolecular) aggregates become more dispersed, releasing DOM through an increase in electrostatic repulsion.³¹ Across the near-neutral to alkaline pH range, this becomes the dominant process controlling the DOC concentration in solution, which is why we name this the "Dissolution Controlled Domain". The dissolution of supramolecular aggregates releases in addition to HA also smaller associated OM fractions into solution, which can be operationally defined as FA and Hy based on their pH-dependent solubility and hydrophobicity properties. Meanwhile, part of these DOM fractions that are released by this dissolution process may adsorb again onto soil minerals, reaching a new equilibrium between adsorbed OM and DOM, explaining the increase in surface-bound OM in this pH range (Figure 4). The transition from the desorption-controlled domain to the dissolution-controlled domain occurs at a lower pH for soils with a high Ca background solution. This indicates that for soils with a high Ca concentration, coagulation/dissolution plays a more important role over a wider pH range, and vice versa. In this conceptual model, pH is considered as a key

factor in determining which process dominates the release of DOM from soil to solution. However, the presence of multivalent cations is also of importance. Multivalent cations such as Ca promote OM coagulation, causing the transition from the desorption-controlled domain to the dissolution-controlled domain to occur at a lower pH. To apply our 4D model to predict the transition from a desorption to dissolution controlled domain in soil, key parameters, including a suitable proxy for soil oxides, RSA, and OM fractions, are required.

A range of land management practices, such as application of lime, biochar, rock powder, and nitrogen fertilizers may influence pH and/or cation concentrations. 67-69 For instance, liming is a common agricultural practice used to counteract soil acidification, which can change both the pH and major cation (e.g., Ca) concentrations. Our findings suggest that a strong increase in the pH of acidic soil may destabilize mineralbound OM, whereas raising the pH of weakly acidic and nearneutral pH soils may predominantly release coagulated OM. The effect of pH on the destabilization of mineral-protected OC is larger for soils with a lower SOC content, leading to further loss of stable carbon. Addition of multivalent cations, as with liming materials, can partially suppress the release of DOM from soil. Our conceptual 4D model gives new insights into the physical-chemical mechanisms that control the solidsolution distribution of OM in soil. Most importantly, our study contributes to a better quantitative understanding of the relative contributions of adsorption/desorption and coagulation/dissolution processes in regulating DOM release under varying soil conditions.

ASSOCIATED CONTENT

5 Supporting Information

The Supporting Information is available free of charge at https://pubs.acs.org/doi/10.1021/acsearthspace-chem.4c00377.

Additional information including (1) properties of selected soil samples, (2) batch experiments, (3) dissolved organic matter fractionation, (4) thermodynamic constants used in the adsorption modeling, (5) soluble Ca and Cu concentrations in the series of batch experiments, (6) flowchart of model calculation, (7) ratio of dissolved organic carbon to soil solid organic carbon, (8) concentrations and proportions of the different DOC fractions, (9) Donnan potential as a function of pH, (10) model coefficients of the fitted broken-line model, (11) relationship between slope and average HA proportion, (12) soluble phosphate concentration, (13) DOC concentration as a functional of Donnan potential, (14) Fraction of surface-bound OM to SOM, (15) soluble Al and Fe concentrations, (16) release of DOM from the dissolution of metal-(hydr)oxides (PDF)

AUTHOR INFORMATION

Corresponding Author

Liping Weng — Agro-Environmental Protection Institute, Ministry of Agricultural and Rural Affairs, Tianjin 300191, China; ocid.org/0009-0006-8045-0141; Email: liping.weng@wur.nl

Authors

Hui Gao — Soil Chemistry Group, Wageningen University & Research, 6708 PB Wageningen, The Netherlands;
orcid.org/0009-0003-1680-5137

Rob N. J. Comans – Soil Chemistry Group, Wageningen University & Research, 6708 PB Wageningen, The Netherlands; © orcid.org/0000-0002-3403-0561

Gerwin F. Koopmans – Soil Chemistry Group, Wageningen University & Research, 6708 PB Wageningen, The Netherlands; orcid.org/0000-0002-3664-6650

Complete contact information is available at: https://pubs.acs.org/10.1021/acsearthspacechem.4c00377

Author Contributions

The manuscript was written through contributions of all authors. All authors have given approval to the final version of the manuscript.

Notes

The authors declare no competing financial interest.

ACKNOWLEDGMENTS

This work was financially supported by the National Key Research and Development Program of China (No. 2023YFD1901305). This work was supported by the Ph.D. scholarship of the China Scholarship Council (CSC). We are also grateful for the accurate and attentive work regarding the sample analysis by Peter Nobels and Johan Uijtenbroek, from the Chemistry and Biology Soil Laboratory (CBLB).

REFERENCES

(1) Zsolnay, Á. Dissolved organic matter: artefacts, definitions, and functions. *Geoderma* **2003**, *113* (3–4), 187–209.

- (2) Guggenberger, G.; Zech, W.; Schulten, H.-R. Formation and mobilization pathways of dissolved organic matter: evidence from chemical structural studies of organic matter fractions in acid forest floor solutions. *Org. Geochem.* **1994**, *21* (1), 51–66.
- (3) Qualls, R. G. Biodegradability of fractions of dissolved organic carbon leached from decomposing leaf litter. *Environ. Sci. Technol.* **2005**, 39 (6), 1616–1622.
- (4) Bolan, N. S.; Adriano, D. C.; Kunhikrishnan, A.; James, T.; McDowell, R.; Senesi, N. Dissolved Organic Matter: Biogeochemistry, Dynamics, and Environmental Significance in Soils. In *Advances in Agronomy*; Elsevier, 2011; Vol. 110, pp 1–75.
- (5) Kaiser, K.; Guggenberger, G. The role of DOM sorption to mineral surfaces in the preservation of organic matter in soils. *Org. Geochem.* **2000**, *31* (7–8), 711–725.
- (6) Kalbitz, K.; Solinger, S.; Park, J.-H.; Michalzik, B.; Matzner, E. Controls on the dynamics of dissolved organic matter in soils: a review. *Soil Sci.* **2000**, *165* (4), 277–304.
- (7) Kindler, R.; Siemens, J. A. N.; Kaiser, K.; Walmsley, D. C.; Bernhofer, C.; Buchmann, N.; Cellier, P.; Eugster, W.; Gleixner, G.; Grünwald, T.; Heim, A.; Ibrom, A.; Jones, S. K.; Jones, M.; Klumpp, K.; Kutsch, W.; Larsen, K. S.; Lehuger, S.; Loubet, B.; McKenzie, R.; Moors, E.; Osborne, B.; Pilegaard, K. I. M.; Rebmann, C.; Saunders, M.; Schmidt, M. W. I.; Schrumpf, M.; Seyfferth, J.; Skiba, U. T. E.; Soussana, J. F.; Sutton, M. A.; Tefs, C.; Vowinckel, B.; Zeeman, M. J.; Kaupenjohann, M. Dissolved carbon leaching from soil is a crucial component of the net ecosystem carbon balance. *Global Change Biol.* **2011**, *17* (2), 1167–1185.
- (8) Ivanic, F. M.; Guggenberger, G.; Woche, S. K.; Bachmann, J.; Hoppe, M.; Carstens, J. F. Soil organic matter facilitates the transport of microplastic by reducing surface hydrophobicity. *Colloids Surf., A* **2023**, *676*, No. 132255, DOI: 10.1016/j.colsurfa.2023.132255.
- (9) Feng, G.; Zhou, B.; Yuan, R.; Luo, S.; Gai, N.; Chen, H. Influence of soil composition and environmental factors on the adsorption of per- and polyfluoroalkyl substances: A review. *Sci. Total Environ.* **2024**, 925, No. 171785.
- (10) Qi, Y.; Cao, H.; Pan, W.; Wang, C.; Liang, Y. The role of dissolved organic matter during Per- and Polyfluorinated Substance (PFAS) adsorption, degradation, and plant uptake: A review. *J. Hazard. Mater.* **2022**, 436, No. 129139.
- (11) Eswaran, H.; Van Den Berg, E.; Reich, P. Organic Carbon in Soils of the World. Soil Sci. Soc. Am. J. 1993, 57 (1), 192–194.
- (12) Kan, Z. R.; Liu, W. X.; Liu, W. S.; Lal, R.; Dang, Y. P.; Zhao, X.; Zhang, H. L. Mechanisms of soil organic carbon stability and its response to no-till: A global synthesis and perspective. *Global Change Biol.* **2022**, *28* (3), 693–710.
- (13) Drake, T. W.; Raymond, P. A.; Spencer, R. G. M. Terrestrial carbon inputs to inland waters: A current synthesis of estimates and uncertainty. *Limnol. Oceanogr. Lett.* **2018**, 3 (3), 132–142.
- (14) Monteith, D. T.; Stoddard, J. L.; Evans, C. D.; de Wit, H. A.; Forsius, M.; Hogasen, T.; Wilander, A.; Skjelkvale, B. L.; Jeffries, D. S.; Vuorenmaa, J.; Keller, B.; Kopacek, J.; Vesely, J. Dissolved organic carbon trends resulting from changes in atmospheric deposition chemistry. *Nature* **2007**, 450 (7169), 537–540.
- (15) Roulet, N.; Moore, T. R. Environmental chemistry: browning the waters. *Nature* **2006**, 444 (7117), 283–284.
- (16) Hruška, J.; Kram, P.; McDowell, W. H.; Oulehle, F. Increased dissolved organic carbon (DOC) in Central European streams is driven by reductions in ionic strength rather than climate change or decreasing acidity. *Environ. Sci. Technol.* **2009**, 43 (12), 4320–4326.
- (17) Nebbioso, A.; Piccolo, A. Molecular characterization of dissolved organic matter (DOM): a critical review. *Anal. Bioanal. Chem.* **2013**, 405 (1), 109–124.
- (18) Shi, S.; Liang, Y.; Jiang, S.; Shi, Z. Improved Predictions of Dissolved Organic Carbon–Water Partitioning and Unveiling the Chemodiversity of Dissolved Organic Matter. ACS Earth Space Chem. **2023**, 7 (6), 1258–1267.
- (19) Van Zomeren, A.; Comans, R. N. J. Measurement of humic and fulvic acid concentrations and dissolution properties by a rapid ratch procedure. *Environ. Sci. Technol.* **2007**, *41*, 6755–6761.

- (20) Kleber, M.; Lehmann, J. Humic Substances Extracted by Alkali Are Invalid Proxies for the Dynamics and Functions of Organic Matter in Terrestrial and Aquatic Ecosystems. *J. Environ. Qual.* **2019**, 48 (2), 207–216.
- (21) Olk, D. C.; Bloom, P. R.; Perdue, E. M.; McKnight, D. M.; Chen, Y.; Farenhorst, A.; Senesi, N.; Chin, Y. P.; Schmitt-Kopplin, P.; Hertkorn, N.; Harir, M. Environmental and Agricultural Relevance of Humic Fractions Extracted by Alkali from Soils and Natural Waters. *J. Environ. Qual.* **2019**, 48 (2), 217–232.
- (22) Gao, H.; Koopmans, G. F.; Song, J.; Groenenberg, J. E.; Liu, X.; Comans, R. N. J.; Weng, L. Evaluation of heavy metal availability in soils near former zinc smelters by chemical extractions and geochemical modelling. *Geoderma* **2022**, 423, No. 115970.
- (23) Van Eynde, E.; Groenenberg, J. E.; Hoffland, E.; Comans, R. N. J. Solid-solution partitioning of micronutrients Zn, Cu and B in tropical soils: Mechanistic and empirical models. *Geoderma* **2022**, 414, No. 115773.
- (24) Gustafsson, J. P. Arsenate adsorption to soils: Modelling the competition from humic substances. *Geoderma* **2006**, *136* (1–2), 320–330.
- (25) Hiemstra, T.; Mia, S.; Duhaut, P. B.; Molleman, B. Natural and pyrogenic humic acids at goethite and natural oxide surfaces interacting with phosphate. *Environ. Sci. Technol.* **2013**, 47 (16), 9182–9189.
- (26) Weng, L.; Van Riemsdiik, W. H.; Hiemstra, T. Effects of fulvic and humic acids on arsenate adsorption to goethite: experiments and modeling. *Environ. Sci. Technol.* **2009**, 43 (19), 7198–7204.
- (27) Weng, L.; Van Riemsdijk, W. H.; Hiemstra, T. Humic nanoparticles at the oxide-water interface: interactions with phosphate ion adsorption. *Environ. Sci. Technol.* **2008**, 42 (23), 8747–8752.
- (28) Koopmans, G. F.; Groenenberg, J. E. Effects of soil oven-drying on concentrations and speciation of trace metals and dissolved organic matter in soil solution extracts of sandy soils. *Geoderma* **2011**, 161 (3–4), 147–158.
- (29) Stevenson, F. J. Humus Chemistry: Genesis, Composition, Reactions; John Wiley & Sons, 1994.
- (30) Filius, J. D.; Hiemstra, T.; Van Riemsdijk, W. H. Adsorption of Small Weak Organic Acids on Goethite: Modeling of Mechanisms. *J. Colloid Interface Sci.* **1997**, *195* (2), 368–380.
- (31) Weng, L.; Temminghoff, E. J. M.; Van Riemsdijk, W. H. Interpretation of humic acid coagulation and soluble soil organic matter using a calculated electrostatic potential. *Eur. J. Soil Sci.* **2002**, 53 (4), 575–588.
- (32) Gerzabek, M. H.; Aquino, A. J. A.; Balboa, Y. I. E.; Galicia-Andrés, E.; Grančič, P.; Oostenbrink, C.; Petrov, D.; Tunega, D. A contribution of molecular modeling to supramolecular structures in soil organic matter. *J. Plant Nutr. Soil Sci.* **2022**, *185* (1), 44–59.
- (33) Sutton, R.; Sposito, G. Molecular structure in soil humic substances: the new view. *Environ. Sci. Technol.* **2005**, 39 (23), 9009–9015.
- (34) Piccolo, A.The Supramolecular Structure of Humic Substances: A Novel Understanding of Humus Chemistry and Implications in Soil Science. In *Advances in Agronomy*; Elsevier, 2002; Vol. 75, pp 57–134.
- (35) Schaumann, G. E. Soil organic matter beyond molecular structure Part I: Macromolecular and supramolecular characteristics. *J. Plant Nutr. Soil Sci.* **2006**, *169* (2), 145–156.
- (36) Benedetti, M. F.; Milne, C. J.; Kinniburgh, D. G.; Van Riemsdijk, W. H.; Koopal, L. K. Metal ion binding to humic substances: application of the non-ideal competitive adsorption model. *Environ. Sci. Technol.* **1995**, 29 (2), 446–457.
- (37) Kinniburgh, D. G.; van Riemsdijk, W. H.; Koopal, L. K.; Borkovec, M.; Benedetti, M. F.; Avena, M. J. Ion binding to natural organic matter: competition, heterogeneity, stoichiometry and thermodynamic consistency. *Colloids Surf.*, A 1999, 151 (1–2), 147–166.
- (38) Van Eynde, E.; Mendez, J. C.; Hiemstra, T.; Comans, R. N. J. Boron adsorption to ferrihydrite with implications for surface speciation in soils: Experiments and modeling. *ACS Earth Space Chem.* **2020**, *4* (8), 1269–1280.

- (39) Mendez, J. C.; Hiemstra, T.; Koopmans, G. F. Assessing the reactive surface area of soils and the association of soil organic carbon with natural oxide nanoparticles using ferrihydrite as proxy. *Environ. Sci. Technol.* **2020**, *54* (19), 11990–12000.
- (40) Osté, L. A.; Temminghoff, E. J.; van Riemsdijk, W. H. Solid-solution partitioning of organic matter in soils as influenced by an increase in pH or Ca concentration. *Environ. Sci. Technol.* **2002**, *36* (2), 208–214.
- (41) Lavallee, J. M.; Soong, J. L.; Cotrufo, M. F. Conceptualizing soil organic matter into particulate and mineral-associated forms to address global change in the 21st century. *Global Change Biol.* **2020**, 26 (1), 261–273.
- (42) Kleber, M.; Eusterhues, K.; Keiluweit, M.; Mikutta, C.; Mikutta, R.; Nico, P. S. Mineral—Organic Associations: Formation, Properties, and Relevance in Soil Environments. In *Advances in Agronomy*; Elsevier, 2015; Vol. 130, pp 1–140.
- (43) Barreto, M. S. C.; Elzinga, E. J.; Ramlogan, M.; Rouff, A. A.; Alleoni, L. R. F. Calcium enhances adsorption and thermal stability of organic compounds on soil minerals. *Chem. Geol.* **2021**, *559*, No. 119804, DOI: 10.1016/j.chemgeo.2020.119804.
- (44) Kaiser, K. Fractionation of dissolved organic matter affected by polyvalent metal cations. *Org. Geochem.* **1998**, 28 (12), 849–854.
- (45) Römkens, P. F. A. M.; Dolfing, J. Effect of Ca on the Solubility and Molecular Size Distribution of DOC and Cu Binding in Soil Solution Samples. *Environ. Sci. Technol.* **1998**, 32 (3), 363–369.
- (46) Kaiser, K.; Kalbitz, K. Cycling downwards—dissolved organic matter in soils. *Soil Biol. Biochem.* **2012**, *52*, 29–32.
- (47) van Erp, P. J.; Houba, Y. J. G.; Van Beusichem, M. L. One hundredth molar calcium chloride extraction procedure. part I: A review of soil chemical, analytical, and plant nutritional aspects. *Commun. Soil Sci. Plant Anal.* 1998, 29 (11–14), 1603–1623.
- (48) Weng, L.; Vega, F. A.; Van Riemsdijk, W. H. Competitive and synergistic effects in pH dependent phosphate adsorption in soils: LCD modeling. *Environ. Sci. Technol.* **2011**, 45 (19), 8420–8428.
- (49) van der Zee, S. E. A. T. M.; van Riemsdijk, W. H. Model for Long-term Phosphate Reaction Kinetics in Soil. *J. Environ. Qual.* **1988**, *17* (1), 35–41.
- (50) Murphy, J.; Riley, J. P. A modified single solution method for the determination of phosphate in natural waters. *Anal. Chim. Acta* **1962**, *27*, 31–36.
- (51) Pribyl, D. W. A critical review of the conventional SOC to SOM conversion factor. *Geoderma* **2010**, *156* (3–4), 75–83.
- (52) Milne, C. J.; Kinniburgh, D. G.; Tipping, E. Generic NICA-Donnan model parameters for proton binding by humic substances. *Environ. Sci. Technol.* **2001**, 35 (10), 2049–2059.
- (53) Milne, C. J.; Kinniburgh, D. G.; van Riemsdijk, W. H.; Tipping, E. Generic NICA-Donnan model parameters for metal-ion binding by humic substances. *Environ. Sci. Technol.* **2003**, *37* (5), 958–971.
- (54) Hiemstra, T.; van Riemsdijk, W. H. Biogeochemical speciation of Fe in ocean water. *Mar. Chem.* **2006**, *102* (3–4), 181–197.
- (55) Hiemstra, T.; Van Riemsdijk, W. H. Surface structural ion adsorption modeling of competitive binding of oxyanions by metal (hydr)oxides. *J. Colloid Interface Sci.* **1999**, 210 (1), 182–193.
- (56) Hiemstra, T.; Van Riemsdijk, W. H. On the relationship between charge distribution, surface hydration, and the structure of the interface of metal hydroxides. *J. Colloid Interface Sci.* **2006**, 301 (1), 1–18.
- (57) Mendez, J. C.; Hiemstra, T. Ternary complex formation of phosphate with Ca and Mg ions binding to ferrihydrite: Experiments and mechanisms. ACS Earth Space Chem. 2020, 4 (4), 545–557.
- (58) Weng, L.; Van Riemsdijk, W. H.; Koopal, L. K.; Hiemstra, T. Ligand and Charge Distribution (LCD) model for the description of fulvic acid adsorption to goethite. *J. Colloid Interface Sci.* **2006**, 302 (2), 442–457.
- (59) Keizer, M. G.; Van Riemsdijk, W. H. A Computer Program for the Equilibrium Calculation of Speciation and Transport in Soil—water Systems. In *Department of Soil Quality*; Wageningen University: Wageningen, 1995.

- (60) Kennedy, J.; Billett, M. F.; Duthie, D.; Fraser, A. R.; Harrison, A. F. Organic matter retention in an upland humic podzol; the effects of pH and solute type. *Eur. J. Soil Sci.* **1996**, *47* (4), 615–625.
- (61) Tipping, E.; Hurley, M. A. A Model of Solid-Solution Interactions in Acid Organic Soils, Based on the Complexation Properties of Humic Substances. *J. Soil Sci.* **1988**, 39 (4), 505–519.
- (62) You, S.-J.; Yin, Y.; Allen, H. E. Partitioning of organic matter in soils: effects of pH and water/soil ratio. *Sci. Total Environ.* **1999**, 227 (2–3), 155–160.
- (63) Kloster, N.; Brigante, M.; Zanini, G.; Avena, M. Aggregation kinetics of humic acids in the presence of calcium ions. *Colloids Surf.*, A **2013**, 427, 76–82.
- (64) Cotrufo, M. F.; Ranalli, M. G.; Haddix, M. L.; Six, J.; Lugato, E. Soil carbon storage informed by particulate and mineral-associated organic matter. *Nat. Geosci.* **2019**, *12* (12), 989–994.
- (65) Xu, Y.; Hiemstra, T.; Tan, W.; Bai, Y.; Weng, L. Key factors in the adsorption of natural organic matter to metal (hydr)oxides: Fractionation and conformational change. *Chemosphere* **2022**, 308 (Pt 1), No. 136129.
- (66) Sowers, T. D.; Adhikari, D.; Wang, J.; Yang, Y.; Sparks, D. L. Spatial Associations and Chemical Composition of Organic Carbon Sequestered in Fe, Ca, and Organic Carbon Ternary Systems. *Environ. Sci. Technol.* **2018**, 52 (12), 6936–6944.
- (67) Li, M.; Wang, J.; Guo, D.; Yang, R.; Fu, H. Effect of land management practices on the concentration of dissolved organic matter in soil: A meta-analysis. *Geoderma* **2019**, *344*, 74–81.
- (68) Luo, Y.; Durenkamp, M.; De Nobili, M.; Lin, Q.; Brookes, P. C. Short term soil priming effects and the mineralisation of biochar following its incorporation to soils of different pH. *Soil Biol. Biochem.* **2011**, 43 (11), 2304–2314.
- (69) Ramos, C. G.; Hower, J. C.; Blanco, E.; Oliveira, M. L. S.; Theodoro, S. H. Possibilities of using silicate rock powder: An overview. *Geosci. Front.* **2022**, *13* (1), No. 101185, DOI: 10.1016/j.gsf.2021.101185.